Superconductivity in Doped sp^3 Semiconductors: The Case of the Clathrates

D. Connétable,[1] V. Timoshevskii,[1] B. Masenelli,[1] J. Beille,[3] J. Marcus,[4] B. Barbara,[3] A. M. Saitta,[2] G.-M. Rignanese,[5]
P. Mélinon,[1] S. Yamanaka,[6] and X. Blase[1]
[1]*LPMCN, Université Claude Bernard Lyon I and CNRS, UMR 5586, Bâtiment Brillouin, 43 Bd du 11 Novembre 1918,*
69622 Villeurbanne Cedex, France
[2]*LPMC, Université Pierre et Marie Curie (Paris 6) and CNRS, UMR 7602, Tour 13/14, 4 Place Jussieu,*
75252 Paris Cedex 05, France
[3]*Laboratoire Louis Néel, CNRS, BP 166, 38042, Grenoble, France*
[4]*LEPES, CNRS, BP 166, 38042, Grenoble, France*
[5]*Université Catholique de Louvain, Unité de Physico-Chimie et de Physique des Matériaux,*
1 Place Croix du Sud, B-1348 Louvain-la-Neuve, Belgium
[6]*Department of Applied Chemistry, Faculty of Engineering, Hiroshima University,*
1-4-1 Kagamiyama, Higashi-Hiroshima, Hiroshima 739-8527, Japan

(Received 21 May 2003; published 8 December 2003)

We present a joint experimental and theoretical study of the superconductivity in doped silicon clathrates. The critical temperature in Ba_8@Si-46 is shown to strongly decrease with applied pressure. These results are corroborated by *ab initio* calculations using MacMillan's formulation of the BCS theory with the electron-phonon coupling constant λ calculated from perturbative density functional theory. Further, the study of I_8@Si-46 and of gedanken pure silicon diamond and clathrate phases doped within a rigid-band approach show that the superconductivity is an intrinsic property of the sp^3 silicon network. As a consequence, carbon clathrates are predicted to yield large critical temperatures with an effective electron-phonon interaction much larger than in C_{60}.

DOI: 10.1103/PhysRevLett.91.247001 PACS numbers: 74.70.Wz, 71.15.Mb, 74.62.Bf, 74.62.Fj

The superconductivity in column-IV elemental compounds has been extensively studied in the case of carbon. In particular, the large observed critical temperature (T_c) in doped C_{60} fullerene networks has stimulated a lot of work [1] while recent theoretical predictions emphasized that by reducing the fullerene size down to C_{36} [2] or even C_{28} [3], T_c could be significantly increased.

Contrary to carbon, silicon does not form sp^2-like networks and, at ambient pressure, there is no superconductivity associated with the sp^3 diamond phase. It is only at higher pressure, upon phase transformation into metallic phases such as the β-tin and simple hexagonal (sh-V) phases at 11 and 13–14 GPa, respectively, that superconductivity with a T_c of 6–8 K could be measured and explained using electron-phonon calculations within the BCS theory [4].

The absence of superconductivity in silicon or carbon sp^3 networks raises the problem of the doping of such dense insulating phases. High doping changes the average lattice constant and introduces mechanical stresses with misfit dislocations [5]. In addition, doping is always limited by the solubility limit for the impurity in the solid which is small at low temperature. Practically, in heavily n-doped silicon, the well known "doping rule limit" predicts [6] a Fermi level located a few tenths of eV above the conduction band minimum (CBM) where the electronic density of states (EDOS) is not large enough to induce superconductivity.

In this perspective, silicon clathrates [7] are promising candidates as they are cagelike materials allowing intercalation. In the case of the type-I clathrates studied here, they are built from a regular arrangement of a combination of Si_{20} (I_h) and Si_{24} (D_{6d}) cages (Fig. 1). Contrary to C_{60} fullerene-assembled films, the silicon cages are strongly linked together since the polyhedra share pentagonal and hexagonal faces. All silicon atoms are thus covalently bonded within a four-neighbor sp^3 environment as in the diamond phase, and silicon clathrates are ~1.8 eV band gap semiconductors [8]. Doping of type-I clathrates leads to a X_8@Si-46 stoichiometry, where X is the in-cage guest atom, displaying thus a huge 8/46 ratio of intercalated to host network atoms. As a result, the Fermi level (E_f) can be strongly displaced in the valence or conduction bands.

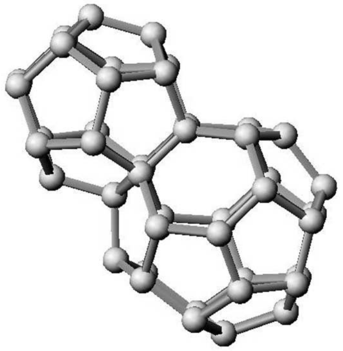

FIG. 1. Symbolic representation of face sharing Si_{20} and Si_{24} cages as a building unit of type-I clathrates.

0031-9007/03/91(24)/247001(4)$20.00

In the case of barium intercalation [9–13], E_f is located around 1 eV above the CBM near a peak in the EDOS related to a hybridization between the Ba-5d orbitals and the Si antibonding states [14]. This has been invoked to be at the origin of the ~8 K superconductivity in Ba_8@Si-46 as reported originally in Ref. [9]. Besides the superconducting properties, these novel phases have recently attracted much attention for the evolution under doping of their pressure-related phase diagram [15], thermoelectric power [16], or band gap [17].

In this Letter, we report on a joint experimental and theoretical study of the superconductivity in doped silicon clathrates. Experimentally, in the case of Ba_8@Si-46, the pressure is found to strongly reduce T_c. These results are reproduced within the BCS theory where the electron-phonon coupling constant λ is calculated *ab initio* from density functional perturbative theory (DFPT) [18]. To understand the origin of the superconductivity in such compounds, the cases of p-doped I_8@Si-46 and empty Si-46 clathrates "artificially doped" within a rigid-band approach are studied on the same theoretical footing. Our results show that the superconductivity is an intrinsic property of the sp^3 silicon network. Further, we predict that the synthesis of carbon clathrates would lead to relatively high T_c compounds.

Ba_8@Si-46 samples were prepared following Ref. [19]. Starting from the $BaSi_2$ Zintl phase mixed with silicon powder and placed in an h-BN cell, the synthesis occurs at 1000 K under high pressure (1–5 GPa). The sample is quenched at room temperature before the pressure is slowly released. The electrical resistivity was measured using a four-wires–type method. Wires were glued with silver varnish and electrical contact improved by annealing. Hydrostatic pressure, up to 18 kbar, was generated in a beryllium-copper self-clamped vessel, in which the samples were pressurized inside a Teflon capsule by a 50/50 pentane-isoamyl alcohol mixture. Pressure was applied at room temperature and the resistivity curves were recorded upon cooling. The reproducibility of the data was checked for each set of measurements, indicating that the sample did not degrade upon pressure or thermal cycling. The superconducting transition temperature T_c is determined at the maximum of the derivative of resistivity versus temperature. As shown in Fig. 2, T_c decreases with pressure. Another doped clathrate labeled Ba_8@Si-40Ag-6 was prepared by substituting some of the silicon atoms by silver. This sample is metalliclike without superconductivity down to 1.5 K.

Our calculations are performed within the local density approximation to the density functional theory [20] and a pseudopotential [21] plane-wave approach. A 16 Ryd energy cutoff and a $2 \times 2 \times 2$ Monkhorst-Pack [22] sampling of the Brillouin zone showed good convergency for structural relaxations. The electron-phonon coupling matrix elements [23], $\langle \psi^0_{n\mathbf{k}} | \hat{\boldsymbol{\epsilon}}_{\mathbf{q}\nu} \cdot (\delta V / \delta \mathbf{R}) | \psi^0_{n\mathbf{k}+\mathbf{q}} \rangle$, were obtained within the framework of DFPT [18]. Because of the computational cost, phonons were calculated at the $\mathbf{q} = \boldsymbol{\Gamma}$ point only. We recall that the unit cell contains 46 silicon and 8 dopants atoms. In particular, two Si_{20} cages are present. Therefore, not only on-ball but also interball phonons are considered within our sampling. Together with the choice of the screened electron-electron interaction μ^* which enters the evaluation of T_c (see below) and the use of the MacMillan formula, this $\mathbf{q}$-point sampling certainly limits the accuracy of the present calculations. We will comment upon this point when comparing our results with the experimental one.

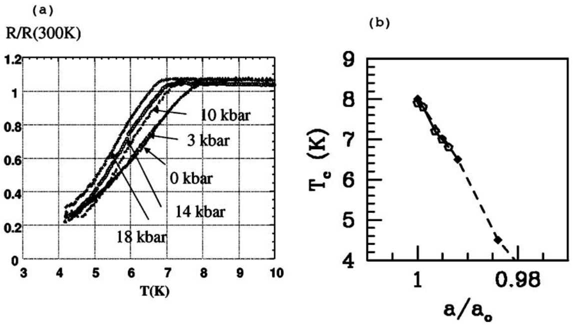

FIG. 2. (a) Evolution of the resistivity (normalized by its value at 300 K) of Ba_8@Si-46 as a function of temperature for different pressures. (b) Evolution of T_c under pressure as a function of the a/a_0 lattice parameter ratio (a_0 ambient pressure lattice parameter). The open circles represent the experimental data and the solid squares the theoretical values. The dashed line is a guide to the eyes.

For the calculation of the variation of the total potential $\delta V / \delta \mathbf{R}$ and of λ,

$$\lambda = N(E_f) V_{ep} = 2N(E_f) \sum_{\nu} \langle\langle |g_{q\nu}|^2 \rangle\rangle / \hbar\omega_{q\nu},$$

where $\langle\langle |g_{\mathbf{q}\boldsymbol{\nu}}|^2 \rangle\rangle$ is related to the $(\mathbf{k}, \mathbf{k}')$ average electron-phonon coupling matrix elements for states over the Fermi surface [23], a larger $8 \times 8 \times 8$ $\mathbf{k}$-point sampling was used. The quantity V_{ep} represents an average electron-phonon interaction strength per electronic state at E_f [with $N(E_f)$ in states/eV]. The knowledge of $\boldsymbol{\lambda}$ allows one to compute T_c following Mac Millan [24]:

$$T_c = \frac{\hbar\omega_{\log}}{1.2k_B} \exp\left[\frac{-1.04(1+\lambda)}{\lambda - \mu^*(1+0.62\lambda)} \right],$$

where $\omega_{\log} = \exp[\sum_{q\nu} \log(\omega_{q\nu}) \lambda_{q\nu} / \sum_{q\nu} \lambda_{q\nu}]$. The value of μ^*, which is the effective electron-electron repulsive interaction, is certainly one of the main problems in the calculation of T_c. In the present work, we adjust μ^* to the value needed to reproduce the $T_c = 8$ K of Ba_8@Si-46 at ambient pressure. For calculations at higher pressure and for different doping (see below), μ^* is kept to be the same [25]. What we seek to reproduce is therefore *the evolution of* T_c either as a function of pressure or as a function of doping. Our fitted value is $\mu^* = 0.24$. This can be compared to the values of ~0.1–0.2 for good elemental metals and to ~0.1–0.3 for C_{60}, C_{36}, and C_{28}.

We compare in Fig. 2 the theoretical and experimental variations of T_c in Ba_8@Si-46 upon pressure. The excellent agreement between theory and experiment concerning this evolution is a solid indication that the BCS theory and our computational framework is able to capture the main physics of such systems. The experimental slope $dT/da = 17.1$ K Å^{-1} is, indeed, close to the theoretical 18.7 K Å^{-1}. We report in Table I the evolution of λ under pressure. The EDOS at the Fermi level, $N(E_f)$, and V_{ep} are found to decrease by ~30% and 20%, respectively, contributing both to the collapse of T_c.

We now try to understand the origin of superconductivity in Ba_8@Si-46. We represent in Fig. 3 the phonon band structure, density of states (pDOS), and coupling constant $\lambda(\omega)$ related to phonons with energy ω only. Contrary to the case of fullerides, where specific on-ball phonon modes were found to be responsible for superconductivity, it is difficult to extract specific phonon and electronic modes with dominant participation to λ.

To gain further insight, we calculate T_c for the p-doped I_8@Si-46 clathrate [17,26]. As shown in Table I, V_{ep} and T_c are very similar to the ones obtained with Ba doping. These results show that superconductivity in doped clathrates is not specifically related to Ba and to the d character of its outer electrons. In the case of Na-doped clathrates, V_{ep} is actually larger than in the case of Ba-doped clathrate, and it is the collapse of $N(E_f)$ which reduces T_c to very small values, in good agreement with experiment.

TABLE I. λ, $N(E_f)$ (states/eV), $\omega_{\log}$ (K), V_{ep} (meV), and T_c (K) as a function of (left column) the reduced lattice parameter a/a_0 for Ba_8@Si-46, different doping elements, and various positions of E_f on the rigid-band model (see text). E_f is given with respect to the top of the valence bands (bottom of the conduction bands) when negative (positive).

a/a_0	λ	$N(E_f)$ (E_f)	V_{ep}	$\langle\omega_{\log}\rangle$	T_c
1.0	1.05	43 (0.9)	24	280	8.4
0.992	0.96	41	23	290	6.9
0.984	0.87	39.5	22	300	4.9
0.969	0.76	37.5	20	314	2.7
0.938	0.58	30	19	326	0.4
Element M					
Na	0.40	15.3 (0.7)	26	360	$\ll 1$
I	0.90	44.4 (− 0.26)	20	300	5.9
E_f	λ	$N(E_f)$	V_{ep}	$\langle\omega_{\log}\rangle$ (K)	T_c (K)
−0.6	1.00	51	19	432	11
−0.4	0.77	23	33	466	4.6
+0.3	0.20	7.4	27	600	0
+0.5	0.41	17.6	23	470	0
+0.7	0.55	20.5	26	405	0.3
+0.9	0.61	26.4	23	366	0.6

In both I and Ba cases, hybridization between Si and intercalated atoms may be interpreted as leading to a coordination which is larger than 4, thus making doped Si clathrates highly coordinated phases equivalent to high-pressure superconducting phases of silicon. To explore this hypothesis, we further calculate T_c for empty clathrates doped within a rigid-band model. Namely, using the $(\delta V/\delta \mathbf{R})$ matrix elements and electronic states calculated for the empty Si-46 phase, the values of λ, $N(E_f)$, and T_c were calculated by locating artificially E_f above or below the band gap, thus allowing the phonons to couple with electronic states at different energies. The results are given in Table I. Again, we find that V_{ep} is rather stable, with values comparable to the one of Ba- or I-doped clathrates, and that the superconductivity is mainly related to $N(E_f)$.

Further, we have performed the same rigid-band analysis in the silicon diamond phase [27]. The coupling constant λ is found to range between 0.4–0.7 for E_f located up to 1 eV above the CBM. With a $\omega_{\log} \sim 450$ K prefactor, and with $\mu^* = 0.24$, the critical temperature is found to be in the {0–5 K} energy range, which compares reasonably well with the clathrate case where we could not find any "cage-related" modes contributing preferentially to λ. These results show that sp^3 silicon networks in general lead intrinsically to a large electron-phonon coupling and that T_c of ~8 K can be obtained provided that sufficient doping is available. These findings are consistent with the collapse of T_c in Ba_8@Si-40Ag-6 compounds where the silver noble metal in substitution in the Si network destroys its sp^3 character.

We now conclude our study by exploring the case of the hypothetical carbon clathrates. As such phases are composed of C_{20} and C_{24} cages, it is tempting to extrapolate the results obtained for free C_{60}, C_{36}, and C_{28} clusters [2,3] which predict an increase of T_c with decreasing sphere radius. However, as in the clathrate phase the cages are sharing faces, such an extrapolation is subject to caution. Nevertheless, the present results suggest that superconductivity can occur in doped sp^3 column-IV

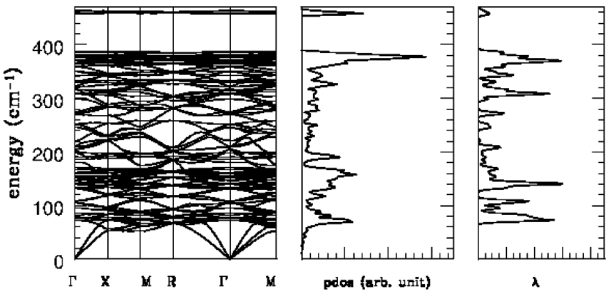

FIG. 3. Phonon band structure, the pDOS of Ba_8@Si-46 at ambient pressure and the coupling constant $\lambda(\omega)$.

materials. Following the rigid-band scheme adopted for silicon clathrates, and with an average phonon frequency $\omega_{\log} \sim 1500$ K, our *ab initio* evaluation of λ yields values as large as 1.4 for E_f located up to 1 eV above the CBM. Our values for V_{ep} range between 150–250 meV which can be compared to the 210 meV found by Breda *et al.* for isolated C_{28} clusters [3]. It is, in particular, much larger than the ~60 meV value found for C_{60} [1], suggesting that purely sp^3 network can be even more efficient in yielding superconductivity than the "curved sp^2 systems" considered so far [28].

In conclusion, we have presented a combined experimental and theoretical study of the superconductivity in doped silicon clathrates. The critical temperature of Ba_8@Si-46 and its decrease under pressure is well reproduced within the BCS theory with electron-phonon coupling constants calculated *ab initio*. Our results show that superconductivity in doped silicon clathrates is an intrinsic property of the sp^3 network and is not specifically related to the Ba-5*d* states or an increase of coordination under doping. As a result, we show that large critical temperatures can be expected for the hypothetical carbon clathrate phases. As shown in Ref. [29], an efficient doping of carbon clathrates could be obtained by Li intercalation or boron substitution.

Calculations have been performed at the French CNRS national computer center at IDRIS (Orsay). X. B. is indebted to P. Quemerais and M. Côté for stimulating discussions.

Note added.—In two recent papers published after submission of our manuscript, our calculated values for λ and μ^* in Ba_8@Si-46 were confirmed experimentally [30], and similar results concerning the prediction of T_c in doped carbon clathrates were obtained [31].

---

[1] O. Gunnarsson, Rev. Mod. Phys. **69**, 575 (1997).
[2] M. Côté, J. C. Grossman, M. L. Cohen, and S. G. Louie, Phys. Rev. Lett. **81**, 697 (1998).
[3] N. Breda *et al.*, Phys. Rev. B **62**, 130 (2000).
[4] K. J. Chang *et al.*, Phys. Rev. Lett. **54**, 2375 (1985).
[5] D. J. Chadi *et al.*, Phys. Rev. Lett. **79**, 4834 (1997); P. H. Citrin *et al.*, Phys. Rev. Lett. **83**, 3234 (1999).
[6] S. B. Zhang, S.-H. Wei, and A. Zunger, Phys. Rev. Lett. **84**, 1232 (2000).
[7] J. S. Kasper *et al.*, Science **150**, 1713 (1965).
[8] E. Galvani *et al.*, Phys. Rev. Lett. **77**, 3573 (1996); J. Gryco *et al.*, Phys. Rev. B **62**, R7707 (2000); X. Blase, Phys. Rev. B **67**, 035211 (2003).
[9] H. Kawaji, H.-O. Horie, S. Yamanaka, and M. Ishikawa, Phys. Rev. Lett. **74**, 1427 (1995).
[10] H. Sakamoto *et al.*, Physica (Amsterdam) **341C**, 2135 (2000).
[11] S. Yamanaka, H. O. Horie, H. Kawaji, and M. Ishikawa, Eur. J. Solid State Inorg. Chem. **32**, 799 (1995).
[12] I. M. Gat *et al.*, Physica (Amsterdam) **289B**, 385 (2000).
[13] Y. Nozue, G. Hosaka, E. Enishi, and S. Yamanaka, Mol. Cryst. Liq. Cryst. **341**, 509 (2000); H. Fukuoka, J. Kiyoto, and S. Yamanaka, Inorg. Chem. **42**, 2933 (2003).
[14] S. Saito and A. Oshiyama, Phys. Rev. B **51**, 2628 (1995); T. Yokoya *et al.*, Phys. Rev. B **64**, 172504 (2001).
[15] A. San Miguel *et al.*, Phys. Rev. Lett. **83**, 5290 (1999); Phys. Rev. B **65**, 054109 (2002); J. S. Tse *et al.*, Phys. Rev. Lett. **89**, 195507 (2002); T. Kume *et al.*, Phys. Rev. Lett. **90**, 155503 (2003).
[16] J. L. Cohn *et al.*, Phys. Rev. Lett. **82**, 779 (1999); J. S. Tse *et al.*, Phys. Rev. Lett. **85**, 114 (2000).
[17] D. Connétable, V. Timoshevskii, E. Artacho, and X. Blase, Phys. Rev. Lett. **87**, 206405 (2001).
[18] S. Baroni, S. de Gironcoli, A. Dal Coso, and P. Giannozzi, Rev. Mod. Phys. **73**, 515 (2001); S. Baroni, A. Dal Corso, S. de Gironcoli, and P. Giannozzi, http://www.pwscf.org.
[19] S. Yamanaka, E. Enishi, H. Fukuoka, and M. Yasukawa, Inorg. Chem. **39**, 56 (2000).
[20] P. Hohenberg and W. Kohn, Phys. Rev. **136**, B864 (1964); D. M. Ceperley and B. J. Alder, Phys. Rev. Lett. **45**, 566 (1980).
[21] N. Troullier and J. L. Martins, Phys. Rev. B **43**, 1993 (1991); L. Kleinman and D. M. Bylander, Phys. Rev. Lett. **48**, 1425 (1982).
[22] H. J. Monkhorst and J. D. Pack, Phys. Rev. B **13**, 5188 (1976).
[23] We follow the notations of M. M. Dacarogna and M. L. Cohen, Phys. Rev. Lett. **55**, 837 (1985).
[24] W. L. McMillan, Phys. Rev. **167**, 331 (1968).
[25] An empirical relation for the variation under pressure of μ^* with $N(E_F)$ is provided in M. M. Dacarogna, M. L. Cohen, and P. K. Lam, Phys. Rev. B **34**, 4865 (1986). With this relation, μ^* does not change by more that 1% between our two extreme values for $N(E_F)$.
[26] E. Rény *et al.*, Phys. Rev. B **66**, 014532 (2002).
[27] The **k**- and **q**-point samplings were increased, respectively, to $30 \times 30 \times 30$ and $6 \times 6 \times 6$ grids.
[28] For free carbon clusters, the increase in sp^3 character with decreasing radius has been often invoked to explain the upward evolution of V_{ep}. Our study confirms that maximizing the sp^3 character of the carbon network increases the electron-phonon coupling.
[29] M. Bernasconi, S. Gaito, and G. Benedek, Phys. Rev. B **61**, 12 689 (2000).
[30] K. Tanigaki *et al.*, Nature Mater. **2**, 653 (2003).
[31] I. Spagnolatti, M. Bernasconi, and G. Benedek, Eur. Phys. J. B **34**, 63 (2003).